Journal of Solid State Chemistry 184 (2011) 859–862

Contents lists available at ScienceDirect

Journal of Solid State Chemistry

journal homepage: www.elsevier.com/locate/jssc

Simple synthesis of mesoporous boron nitride with strong cathodoluminescence emission

Xiang-Lin Meng, Ning Lun, Yong-Xin Qi, Hui-Ling Zhu, Fu-Dong Han, Long-Wei Yin, Run-Hua Fan, Yu-Jun Bai *, Jian-Qiang Bi *

Key Laboratory for Liquid-Solid Structural Evolution and Processing of Materials, Ministry of Education, Shandong University, Jinan 250061, PR China

ARTICLE INFO

Article history:
Received 8 September 2010
Received in revised form
22 January 2011
Accepted 31 January 2011
Available online 20 February 2011

Keywords:
Boron nitride
Nanostructure
Density functional theory

ABSTRACT

Mesoporous BN was prepared at 550 °C for 10 h or so via a simple reaction between $NaBH_4$ and $CO(NH_2)_2$. X-ray diffraction demonstrates the formation of t-BN with lattice constants $a=2.46$ and $c=6.67$ Å. High-resolution transmission electron microscopy displays a lot of porous films in the product, which possesses a high surface area of 219 $m^2\,g^{-1}$ and a pore size primarily around 3.8 nm tested by nitrogen adsorption–desorption method. The mesoporous BN exhibits a strong luminescence emission around 3.41 eV in the cathodoluminescence spectra, a high stability in both morphology and structure, and good oxidation resistance up to 800 °C. The byproducts generated during the reaction are responsible for the formation of the mesoporous BN.

1. Introduction

Porous materials are extensively used as catalyst supports, gas adsorbents, sensors, for chemical purification and separation due to their high surface area and high porosity [1–9]. Traditional porous oxide supports such as Al_2O_3, SiO_2, and zeolite have been widely utilized, whereas the low thermal conductivity and high sensibility to moisture may sometimes result in some disadvantages, such as causing severe metal sintering on the hot spots, and making the catalyst be covered with water at low temperature [10–13]. Activated carbon is another economical porous solid that has been widely employed [14]. However, carbon materials can be easily oxidized in air atmosphere above 300 °C [15], restricting their applications under oxidative atmosphere at high temperatures.

Boron nitride (BN) has some unique properties, such as high thermal conductivity, hydrophobility, good optical properties, excellent resistance to chemical attack and high stability towards oxidation [4,5,12,15], making porous BN particularly applicable as gas absorbents [4,5], and catalyst supports at high temperatures under harsh conditions [6,7,16,17]. Recently, the preparation of porous BN has received growing attention. Templating method is so far the most common route to fabricate porous BN using carbon or silica as templates. Disordered porous BN [18] and ordered BN mesostructure [19,20] were obtained using activated carbon and carbon molecular sieves as templates, respectively. Mesoporous BN was synthesized at temperatures above 1150 °C using mesoporous carbon [1,16] or silica as templates [21]. Though the porous BN obtained by the templating method possesses relatively high surface areas, the high reaction temperature and intricate processing are the main drawbacks that embarrass the mass production of the porous BN with low cost. Pyrolysis of borane-based molecular precursors has also been adopted to fabricate porous BN. Borek et al. [4] produced porous BN by vacuum pyrolysis of poly (4, 6-borazinylamine) at 600–1200 °C. Lindquist et al. [22] fabricated BN aerogels which exhibited excellent thermal stability even when heated to 1500 °C in argon atmosphere. Wood and Paine [23] synthesized hollow spherical BN, and spherical BN powders [24] beyond 800 °C. BN foams were prepared by thermolyzing molecular precursors up to 1800 °C [19] or from borane hydrazine by self-propagating high-temperature synthesis [25]. Several other approaches have also been reported. Lin et al. [26] synthesized h-BN powders with a surface area of 152 $m^2\,g^{-1}$ at 1000 °C using KBH_4, NH_4Cl and KCl as reagents. In view of the present researches, it is of great significance to explore some simple approaches to the porous BN with high surface areas at relatively low temperatures.

As has been known, BN is a promising material for optoelectronic applications. The first observation of an intense far-ultraviolet (UV) excition emission enables BN to be employed in new light-emitting devices [27,28], and thus has attracted increasing interest in recent years. Cathodoluminescence (CL) spectroscopy is an effective method to measure the optical property of BN with

* Corresponding author. Fax: +86 531 88392315.
E-mail addresses: byj97@126.com (Y.-J. Bai), bjq1969@163.com (J.-Q. Bi).

0022-4596/$ - see front matter © 2011 Elsevier Inc. All rights reserved.
doi:10.1016/j.jssc.2011.01.040

various morphologies. The spectra of BN nanosheets were reported to be between 3.79 and 3.96 eV owing to deep-level emissions associated with defect-related centers [29]. The CL spectra of BN nanoribbons are centered at 5.33 eV [30]. For BN nanotubes, Zhi et al. [31] reported a strong CL peak located around 3.3 eV and a weak peak at 4.1 eV resulted from the defects, or B and N vacancies. Han et al. [32] also reported the CL spectra of BN nanotubes to be between 3.0 and 4.2 eV. However, to the best of our knowledge, it is presently almost unknown about the CL property of porous BN.

In this work, we reported a convenient route to synthesize mesoporous BN at 550 °C or so in the absence of additional templates using the commonly available cheap reagents of urea ($CO(NH_2)_2$) and sodium borohydride ($NaBH_4$) as raw materials. The mesoporous BN obtained exhibits a large specific surface area of 219 $m^2\ g^{-1}$, a strong luminescence emission around 3.41 eV, a high stability in both morphology and structure, and excellent oxidation resistance up to 800 °C.

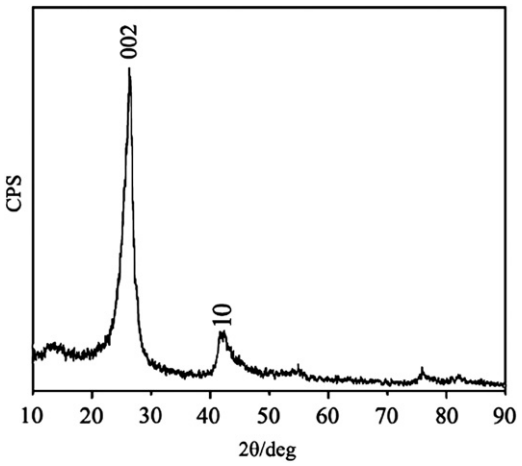

Fig. 1. XRD pattern of the resulting product.

2. Experimental

Analytically pure $CO(NH_2)_2$ (produced by Tianjin Chemical Reagent No. 1 Plant, Tianjin, PR China) and $NaBH_4$ (produced by Zhanyun Chemical Co. Ltd., Shanghai, PR China) were used as starting materials. In a typical procedure, 1.53 g (0.041 mol) $NaBH_4$ and 1.54 g (0.026 mol) $CO(NH_2)_2$ were mixed and put into a stainless steel autoclave with a capacity of 30 mL. Then the autoclave was sealed and heated at a rate of 20 °C/min in furnace to 550 °C and maintained for 10 h. When the autoclave was cooled to ambient temperature naturally, the products in the autoclave were collected and washed successively with anhydrous ethanol, dilute hydrochloric acid and distilled water several times to eliminate the residual reagents and byproducts. The final product was dried at 60 °C for 10 h and white powders were ultimately obtained. The yield of the resulting product was about 65 wt% based on the starting material of $NaBH_4$.

X-ray powder diffraction (XRD) patterns were obtained on a Rigaku Dmax-rc diffractometer with Ni-filtered Cu $K\alpha$ radiation (V=50 kV, and I=80 mA) at a scanning rate of 4°/min. The morphology of the products was examined using a Tecnai 20U-Twin high-resolution TEM (HRTEM) with a point-to-point resolution of 0.19 nm operating at 200 kV. A CL spectrophotometer attached to a SU-70 type thermal field emission scanning electron microscope (FESEM) was used to investigate the optical properties of the samples.

Nitrogen adsorption–desorption isotherms were carried out at 77.3 K on a Quadrasorb SI sorption analyzer. The samples were outgassed for 8 h at 300 °C under a vacuum in the degas port of the analyzer. The specific surface area was calculated with the Brunauer–Emmett–Teller (BET) model, and pore size distribution was calculated from the adsorption–desorption data using the Density Functional Theory (DFT) method.

3. Results and discussion

Fig. 1 shows the XRD pattern of the resulting product obtained from the reaction of $NaBH_4$ and $CO(NH_2)_2$ at 550 °C for 10 h, which is in good agreement with those described in literature for t-BN [33–36]. The diffraction peak at 2θ=26.7° can be indexed to the (0 0 2) plane, indicative of the presence of layered structure in the t-BN. The peak at 2θ=42.4° corresponds to the (10) plane (unresolved (1 0 0) and (1 0 1) planes for h-BN). Owing to the partially disordered lattice, t-BN does not have an accurate crystal structure, and its lattice constants are usually determined by referring to h-BN. The lattice constants of the t-BN obtained are a=2.46 Å and c=6.67 Å, which agree well with the values reported in literature [33].

A Bruker Vertex 70 spectrometer was used to obtain Fourier transformation infrared spectra of the resulting products (Fig. S1 in supporting information). Two strong characteristic absorption peaks at 1379 and 800 cm^{-1} give further confirmation for the formation of t-BN [34,37].

The morphology of the products was investigated by HRTEM, as shown in Fig. 2. Thin films about 20–30 nm in thickness and 0.4–0.6 μm^2 in areas are the dominant morphology. A mass of disordered pores with diameters of 3–5 nm can be observed throughout the films. The inset in Fig. 2a is the lattice fringe image of one piece of the films, the average distance between the neighboring fringes is about 0.34 nm which is consistent with the spacing of (0 0 2) plane of t-BN. In order to understand the stability of the porous BN, the as-prepared product was heated in air to 700 °C and held at this temperature for 1.5 h. Fig. 2b displays the HRTEM image of the heat-treated product, from which the porous structure is almost the same as that in Fig. 2a, and the lattice spacing is still about 0.34 nm, confirming the high stability of the porous BN in both morphology and structure. The structure stability was also supported by XRD characterization, which is shown in Fig. S2 in supporting information.

The luminescence property of the porous BN was examined by FESEM equipped with a CL spectrophotometer. Fig. 3 exhibits the FESEM image of the product and the corresponding room temperature CL spectrum. The porous BN displays a strong CL behavior in UV range. The broad emission peaks around 364 and 522 nm in the spectrum correspond to the energy of 3.41 and 2.38 eV, respectively. It is obvious that the emissions are greatly different from those resulted from pure h-BN single crystal with perfect crystallinity (215 nm) [27,28], but are similar to those from BN nanosheets (3.79–3.96 eV) [29], and BN nanotubes (3.0–4.2 eV) [31,32]. Comparing with the emission of pure h-BN single crystal, the shift of emission could be attributed to the significant difference in crystallinity, of course, other factors such as impurities, defects, or B and N vacancies are also inevitable [31,38]. For the porous BN, the CL peaks around 3.41–2.38 eV could also be ascribed to the deep-level emissions associated with the defect-related centers (B or N vacancy type defect trapped states [29,38,39]), because more defects may occur in the porous structure with large surface areas.

The BET surface area and pore-size distribution of the porous BN were characterized by nitrogen adsorption–desorption isotherms, as shown in Fig. 4. The isotherms exhibit a hysteresis loop

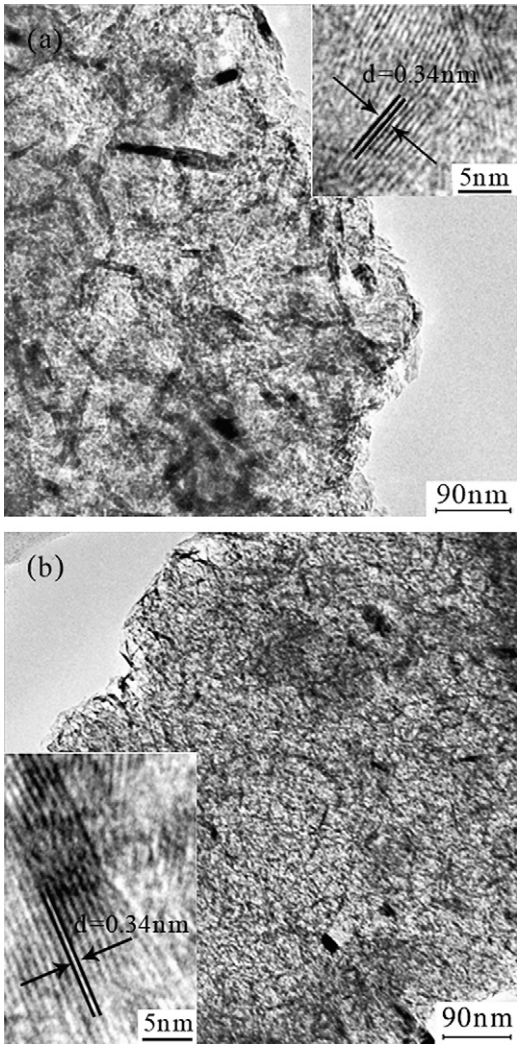

Fig. 2. HRTEM images of the as-prepared product (a) and the product heat-treated in air at 700 °C for 1.5 h (b). The insets in (a) and (b) are the lattice fringe images of the corresponding products.

at a relative pressure between 0.45 and 0.95, suggesting the formation of mesoporous BN [40]. The surface area and pore capacity of the porous BN calculated from Fig. 4a are 219 $m^2 g^{-1}$ and 0.32 $cm^3 g^{-1}$, respectively. From Fig. 4b, the pore-size distribution is dominant between 1 and 5 nm with an average pore size of 3.8 nm.

For better understanding the thermal stability and oxidation resistance of the mesoporous BN, combined DTA–TGA analysis was conducted in a SDT Q600 thermal-microbalance apparatus (TA Instruments Ltd., New Castle, Delaware) at a heating rate of 10 °C/min in air atmosphere using Al_2O_3 pans. The TGA–DTA curves between room temperature and 1200 °C (Fig. S3 in supporting information) demonstrate that the mesoporous BN has good thermal stability and oxidation resistance up to 800 °C. Associated with the morphology depicted in Fig. 2c, besides the high stability in morphology and structure, the mesoporous BN is oxidation resistant up to 800 °C, and thus can be utilized as gas absorbents and catalyst supports at high temperatures under harsh conditions.

To probe into the effect of reaction temperature and time on the formation of the mesoporous BN, a series of experiments were conducted. When the temperature is lower than 450 °C, the reaction between $NaBH_4$ and $CO(NH_2)_2$ cannot occur, and no BN can be achieved. When the temperature is above 600 °C, the

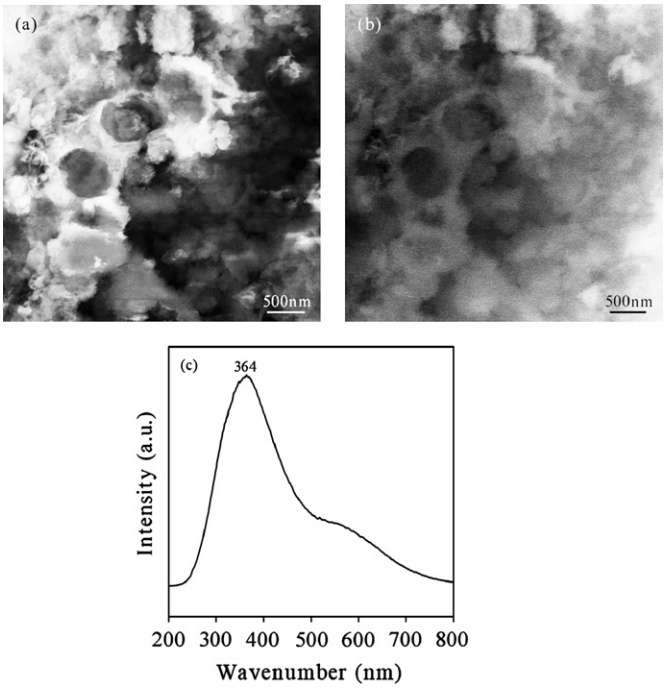

Fig. 3. FESEM image (a), the corresponding CL image (b) and CL spectrum (c) of the porous BN.

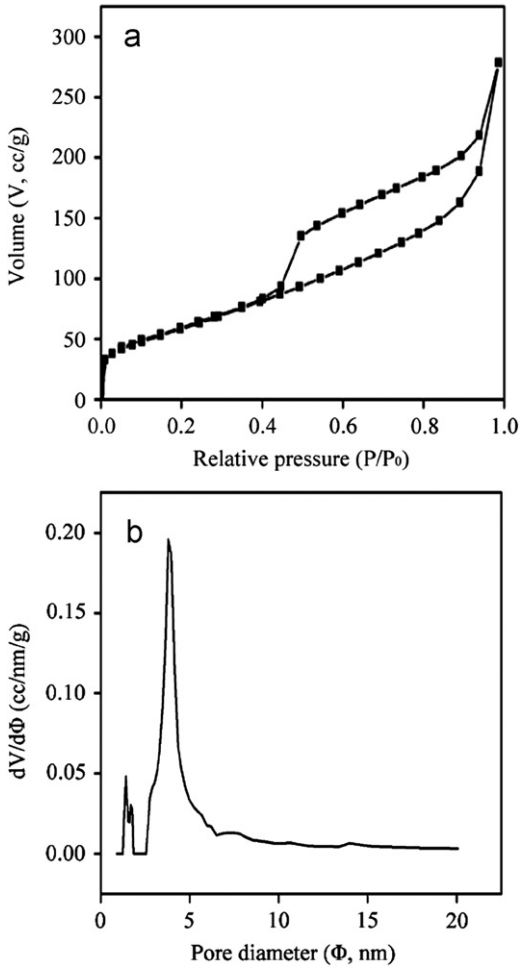

Fig. 4. Nitrogen adsorption–desorption isotherms (a) and DFT pore-size distribution curve (b) determined from the nitrogen desorption isotherm of the mesoporous BN.

porous structure hardly changes both in yield and in morphology. If the holding time is less than 6 h at 550 °C, the reaction is incomplete and the crystallinity of BN is poorer. The reaction time over 10 h does not significantly influence the crystallization and the yield of the mesoporous BN.

According to the XRD pattern of the as-prepared product without any washing treatments (Fig. S4 in supporting information), besides BN, NaCN is also present in the product (Caution: NaCN is toxic and should be carefully processed). In addition, when the autoclaves were opened after the reaction, some gases gave out, which may involve NH_3, H_2, and CO_2 [41,42]. Consequently, the possible reaction can be expressed as follows:

$$2CO(NH_2)_2 + NaBH_4 = BN + NaCN + 2NH_3 + CO_2 + 3H_2$$

With the rise of temperature, $CO(NH_2)_2$ starts to decompose beyond its melting point (132.7 °C) and generate gases of HCNO and NH_3 [43]. Then HCNO reacts with $NaBH_4$ to yield NaCN, borane and H_2O ($\Delta_f G = -106.72$ kJ/mol), and borane combines subsequently with NH_3 to form borazine around 200 °C [44]. Under the autogenic pressure and the reaction temperature of 550 °C or so, borazine pyrolyzes into BN and hydrogen [42]. The byproducts of NaCN and the gases produced during the reaction may act as the templates for the formation of the mesoporous BN. When the byproducts were washed away, t-BN with mesoporous structure was ultimately remained.

4. Conclusions

In summary, mesoporous BN could be synthesized by the simple reaction between $NaBH_4$ and $CO(NH_2)_2$ at 550 °C for 10 h without using additional templates. The mesoporous structure with a large surface area of 219 $m^2\,g^{-1}$ and a pore size distribution primarily around 3.8 nm exhibits a strong luminescence emission around 3.41 eV in the CL spectra, a high thermal stability in both morphology and structure, and good oxidation resistance up to 800 °C. The cheap reactants of $CO(NH_2)_2$ and $NaBH_4$, and the easy operation make this convenient route applicable in large-scale synthesis of mesoporous BN utilized as high temperature gas absorbents and catalyst supports under harsh conditions.

Acknowledgments

This work was supported by the National Natural Science Foundation of China (Nos. 50972076 and 50872072), Shandong Provincial Natural Science Foundation, PR China (Nos. Y2008F26 and Y2008F40), Science and Technology Development Project of Shandong Province (Nos. 2009GG10003001, 2009GG10003003), and Special Fund for Postdoctoral Innovative Project of Shandong Province (No. 200702024).

Appendix A. Supplementary material

Supplementary data associated with this article can be found in the online version at doi:10.1016/j.jssc.2011.01.040.

References

[1] A. Vinu, M. Terrones, D. Golberg, S. Hishita, K. Ariga, T. Mori, Chem. Mater. 17 (2005) 5887.
[2] C.-G. Wu, T. Bein, Science 266 (1994) 1013.
[3] A.A. Zakhidov, R.H. Baughman, Z. Iqbal, C. Cui, I. Khayrullin, S.O. Dantas, J. Marti, V.G. Ralchenko, Science 282 (1998) 897.
[4] T.T. Borek, W. Ackerman, D.W. Hua, R.T. Paine, D.M. Smith, Langmuir. 7 (1991) 2844.
[5] J.F. Janik, W.C. Ackerman, R.T. Paine, D.W. Hua, A. Maskara, D.M. Smith, Langmuir. 10 (1994) 514.
[6] G. Postole, A. Gervasini, C. Guimon, A. Auroux, B. Bonnetot, J. Phys. Chem. B. 110 (2006) 12572.
[7] J.A. Perdigon-Melon, A. Auroux, C. Guimon, B. Bonnetot, J. Solid State Chem. 117 (2004) 609.
[8] M.E. Davis, Nature 417 (2002) 813.
[9] L.C. Wang, L.Q. Xu, C.H. Sun, Y.T. Qian, J. Mater. Chem. 19 (2009) 1989.
[10] J.A. Perdigon-Melon, A. Auroux, D. Cornu, P. Miele, B. Toury, B. Bonnetot, J. Org. Chem. 657 (2002) 98.
[11] G. Postole, M. Caldararu, N.I. Ionescu, B. Bonnetot, A. Auroux, C. Guimon, Thermochim. Acta. 434 (2005) 150.
[12] J.C.S. Wu, Y.C. Fan, C.A. Lin, Ind. Eng. Chem. Res. 42 (2003) 3225.
[13] M. Caldararu, G. Postole, C. Hornoiu, V. Bratan, M. Dragan, N.I. Ionescu, Appl. Surf. Sci. 181 (2001) 255.
[14] R.C. Bansal, J.B. Donnet, F. Stoeckli, Active Carbons Marcel Dekker, New York and Basel, 1988.
[15] J.C.S. Wu, Z.A. Lin, J.W. Pan, M.H. Rei, Appl. Catal. A—Gen. 219 (2001) 117.
[16] P. Dibandjo, F. Chassagneux, L. Bois, C. Sigala, P. Miele, J. Mater. Res. 22 (2007) 26.
[17] P. Dibandjo, L. Bois, F. Chassagneux, J.M. Letoffe, P. Miele, J. Porous. Mater. 15 (2008) 13.
[18] W.Q. Han, R. Brutchey, T.D. Tilley, A. Zettl, Nano Lett. 4 (2004) 173.
[19] P. Dibandjo, L. Bois, F. Chassagneux, D. Cornu, J.M. Letoffe, B. Toury, F. Babonneau, P. Miele, Adv. Mater. 17 (2005) 571.
[20] P. Dibandjo, F. Chassagneux, L. Bois, C. Sigala, P. Miele, J. Mater. Chem. 15 (2005) 1917.
[21] B. Rushton, R. Mokaya, J. Mater. Chem. 18 (2008) 235.
[22] D.A. Lindquist, T.T. Borek, S.J. Kramer, C.K. Narula, G. Johnston, R. Schaeffer, D.M. Smith, R.T. Paine, J. Am. Ceram. Soc. 73 (1990) 757.
[23] G.L. Wood, R.T. Paine, Chem. Mater. 18 (2006) 4716.
[24] G.L. Wood, J.F. Janik, E.A. Pruss, D. Dreissig, W.J. Kroenke, T. Habereder, H. Noth, R.T. Paine, Chem. Mater. 18 (2006) 1434.
[25] I.P. Borovinskaya, V.A. Bunin, A.G. Merzhanov, Mendeleev. Commun. 7 (1997) 47.
[26] L.X. Lin, Z.H. Li, Y. Zheng, K.M. Wei, J. Am. Ceram. Soc. 92 (2009) 1347.
[27] K. Watanabe, T. Taniguchi, H. Kanda, Nat. Mater. 3 (2004) 404.
[28] Y. Kubota, K. Watanabe, O. Tsuda, T. Taniguchi, Science 317 (2007) 932.
[29] R. Gao, L.W. Yin, C.X. Wang, Y.X. Qi, N. Lun, L.Y. Zhang, Y.X. Liu, L. Kang, X.F. Wang, J. Phys. Chem. C. 113 (2009) 15160.
[30] Z.G. Chen, J. Zou, G. Liu, F. Li, Y. Wang, L.Z. Wang, X.L. Yuan, T. Sekiguchi, H.M. Cheng, G.Q. Lu, ACS Nano 2 (2008) 2183.
[31] C.Y. Zhi, Y. Bando, C. Tang, D. Golberg, R. Xie, T. Sekigushi, Appl. Phys. Lett 86 (2005) 213100–213101.
[32] W.Q. Han, H.G. Yu, C. Zhi, J. Wang, Z. Liu, T. Sekiguchi, Y. Bando, Nano Lett. 8 (2008) 491.
[33] B. Yao, Z.X. Shen, L. Liu, W.H. Su, J. Phys.:Condens. Matter 16 (2004) 2181.
[34] E.J.M. Hamilton, S.E. Dolan, C.M. Mann, H.O. Colijn, S.G. Shore, Chem. Mater. 7 (1995) 111.
[35] Q.X. Guo, Y. Xie, C.Q. Yi, L. Zhu, P. Gao, J. Solid. State. Chem. 178 (2005) 1925.
[36] J.B. Lian, T. Kim, X.D. Liu, J.M. Ma, W.J. Zheng, J. Phys. Chem. C. 113 (2009) 9135.
[37] M.I. Baraton, T. Merle, P. Quintard, V. Lorenzelli, Langmuir. 9 (1993) 1486.
[38] C.Y. Zhi, Y. Bando, C.C. Tang, D. Golberg, Appl. Phys. Lett. 87 (2005) 063107-1.
[39] L.W. Yin, Y. Bando, D. Golberg, A. Gloter, M.S. Li, X.L. Yuan, T. Sekiguchi, J. Am. Chem. Soc. 127 (2005) 16354.
[40] K.S.W. Sing, D.H. Everett, R.A.W. Haul, W. Haul, L. Moscou, R.A. Pierotti, J. Rouquerol, T. Siemieniewska, Pure Appl. Chem. 57 (1985) 603.
[41] A. Roda, F. Piazza, P. Pasini, M. Baraldini, L. Zambonin, S. Fossi, F. Bazzoli, E. Roda, Anal. Biochem. 264 (1998) 47.
[42] S.I. Hirano, T. Yogo, S. Asada, S. Naka, J. Am. Ceram. Soc. 72 (1989) 66.
[43] K. Raidongia, A. Nag, K.P.S.S. Hembram, U.V. Waghmare, R. Datta, C.N.R. Rao, Chem. Eur. J. 16 (2010) 149.
[44] R.T. Paine, C.K. Narula, Chem. Rev. 90 (1990) 73.